Proceedings of the 2003 IEEE/RSJ
Intl. Conference on Intelligent Robots and Systems
Las Vegas, Nevada · October 2003

Human-like Motion of a Humanoid Robot Arm Based on a Closed-Form Solution of the Inverse Kinematics Problem

T. Asfour and R. Dillmann
Industrial Applications of Informatics and Microsystems (IAIM)
Computer Science Department, University of Karlsruhe
Haid-und-Neu-Str. 7, 76131 Karlsruhe
Germany

Abstract— **Humanoid robotics is a new challenging field. To cooperate with human beings, humanoid robots not only have to feature human-like form and structure but, more importantly, they must possess human-like characteristics regarding motion, communication and intelligence. In this paper, we propose an algorithm for solving the inverse kinematics problem associated with the redundant robot arm of the humanoid robot ARMAR. The formulation of the problem is based on the decomposition of the workspace of the arm and on the analytical description of the redundancy of the arm. The solution obtained is characterized by its accuracy and low cost of computation. The algorithm is enhanced in order to generate human-like manipulation motions from object trajectories.**

I. INTRODUCTION

From the mechanical point of view, a robot arm imitating the human arm motions should be kinematically redundant like the human arm. According to [1], the human arm mechanism is composed of seven degrees of freedom (DOF) from the shoulder to the wrist. Because there is kinematic redundancy, an infinite number of joint angle trajectories leads to the same end-effector trajectory. Kinematics redundancy can be used to avoid joint limits [2], obstacles [3], and singular configurations [4], as well as to provide a fault tolerant operation [5] or to optimize the robot arm dynamics [6]. Standard methods that deal with redundancy can be divided in two global and local methodes [7]. The former require prior information about the entire Cartesian space trajectory of the end-effector to generate, usually iteratively, a set of joint angle trajectories with global optimality. Therefore, global control schemes are computationally expensive and not suitable for real-time implementation. On the other hand, local methods use only the instantaneous position of the end-effector to perform local optimization in real time. Therefore, local control schemes are required in case of cooperation tasks between humans and humanoid robots.

The use of redundancy for the generation of human-like robot arm motions has been already proposed in the literature and a variety of hypothetical cost functions has been suggested to explain principles of the human arm movements [8]. In [9], for instance, the kinematic redundancy is used to achieve human-like joint motions of a robot arm during the writing task. Recently, human motion capture has been used for the generation of kinematics models describing human and humanoid robot motions [10]. This method has been successfully applied to the generation of human-like motions of our humanoid robot ARMAR [11]. However, the applicability of this method to generate human-like manipulation motions is not yet clear from the literature.

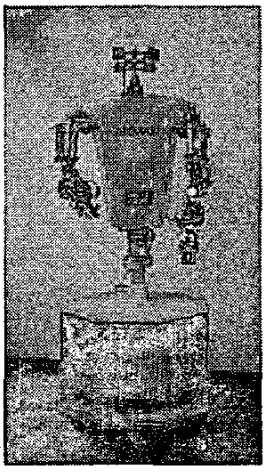

Fig. 1. The humanoid robot ARMAR

In this paper we consider the problem of generating human-like motions from the kinematics point of view. We rely on a hypothesis from neurophysiology and present its on-line application for generating human-like motions of a redundant humanoid robot arm. The paper is organized as follows. Section II describes the kinematics of the 7-DOF arm of the humanoid robot ARMAR. The description of the arm redundancy and the algorithm for solving the inverse kinematics problem is given in section III. Section IV presents the approach we use to generate human-like motions. Finally section V summarizes the results and concludes the paper.

0-7803-7860-1/03/$17.00 © 2003 IEEE

II. THE KINEMATICS MODEL OF THE ARM

Figure 2 shows the reference and link coordinate systems of the 7-DOF arm using the Denavit-Hartenberg convention. The values of the kinematic parameters are listed in table I, where l_s, l_u and l_f are the link lengths of shoulder, upperarm and forearm, respectively. They correspond to the home position pictured in the link coordinate diagram of figure 2. The Denavit-Hartenberg convention

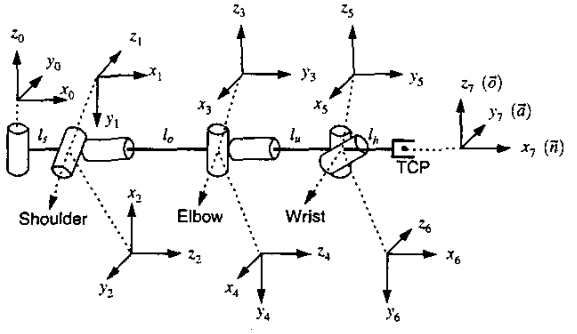

Fig. 2. Coordinate systems of the arm

allows the construction of the forward kinematics function by composing the coordinate transformations into one homogeneous transformation matrix. The description of the coordinate transformation between frame i and frame $i-1$ is given by the homogeneous transformation matrix

$$A_i = \begin{pmatrix} c_{\theta_i} & -c_{\alpha_i}s_{\theta_i} & s_{\alpha_i}s_{\theta_i} & a_i c_{\theta_i} \\ s_{\theta_i} & c_{\alpha_i}c_{\theta_i} & -s_{\alpha_i}c_{\theta_i} & a_i s_{\theta_i} \\ 0 & s_{\alpha_i} & c_{\alpha_i} & d_i \\ 0 & 0 & 0 & 1 \end{pmatrix}, \qquad (1)$$

where s_{η_i} and c_{η_i} are $\sin\eta_i$ and $\cos\eta_i$, respectively. Having defined a frame for each link, the coordinate transformation describing the position and orientation of the end-effector with respect to the base frame is given by

$$T_{tcp}(\vec{\theta}) = \prod_{i=1}^{7}(A_i(\theta_i)) = \begin{pmatrix} \vec{n} & \vec{o} & \vec{a} & \vec{p} \\ 0 & 0 & 0 & 1 \end{pmatrix}, \qquad (2)$$

TABLE I
DENAVIT-HARTENBERG PARAMETERS OF THE ARM

i	θ_i	α_i	$a_i[mm]$	$d_i[mm]$	range
1	θ_1	$-90°$	l_s	0	$-90°\cdots 90°$
2	$\theta_2-90°$	$-90°$	0	0	$-90°\cdots 90°$
3	$\theta_3+90°$	$90°$	0	l_u	$-230°\cdots 90°$
4	θ_4	$-90°$	0	0	$0\cdots 145°$
5	θ_5	$90°$	0	l_f	$0\cdots 350°$
6	$\theta_6+90°$	$-90°$	0	0	$-45°\cdots 45°$
7	θ_7	$90°$	l_h	0	$45°\cdots 45°$

where $\vec{\theta}$ is the (7×1) vector of the joint variables, $\vec{n}, \vec{o}$ and $\vec{a}$ are the unit vectors of the frame attached to the end-effector, and $\vec{p}$ is the position vector of the origin of this frame with respect to the origin of the reference frame (x_0, y_0, z_0) (figure 2).

III. THE REDUNDANCY OF THE ARM

The robot arm redundancy can be described by the rotation of the center of the elbow joint about the axis, that passes through the wrist and the origin of the base frame (x_0, y_0, z_0). The feasible positions of the elbow around this axis are defined by a curve. This curve can be derived from the fact that the ending point of the upper arm describes an ellipsoid centered in the origin of the base coordinate system (x_0, y_0, z_0) and that the starting point of the forearm describes a sphere centered on the wrist (x_w, y_w, z_w), which corresponds to the origin of the coordinate system (x_6, y_6, z_6) in figure 2. Since these two points have to coincide, the redundancy curve results from the intersection of the ellipsoid and the sphere. Figure 3 shows the ellipsoid, which is given by

$$\frac{x}{(l_s+l_o)^2} + \frac{y}{(l_s+l_o)^2} + \frac{z}{(l_o)^2} = 1\,. \qquad (3)$$

and the sphere with the radius l_f and whose center is given by the position vector $\vec{w}$ of the wrist

$$\vec{w} = (x_w, y_w, z_w)^T = \vec{p} - l_h \cdot \vec{n}, \qquad (4)$$

where $\vec{p}$ is the position vector of the end-effector, l_h is the distance between the wrist and $\vec{n}$ the normal vector of the frame attached to the end-effector (figure 2). For a given position and orientation of the end-effector all possible positions of the elbow (x_e, y_e, z_e) can be determined based on the derived description of the arm redundancy. Once having the elbow position and orientation (both the origin and the unit vectors of the coordinate system (x_4, y_4, z_4)), the remaining joint angles are then easy to determine.

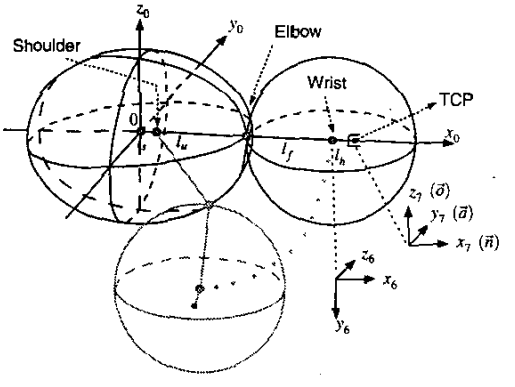

Fig. 3. Workspace of the upperarm and forearm

The description of the complete curve resulting from the intersection of the ellipsoid and the sphere mentioned above is analytically difficult. To make this task mathematically tractable, we first determine the intersection between the ellipsoid and the sphere at $z = z_e$. The redundancy curve of the arm can eventually be obtained by combining all such intersections for all values of z_e in the interval $[z_e^{min}, z_e^{max}]$, where z_e^{min} and z_e^{max} are the minimal and maximal values of the z-coordinate of the elbow for a given position and orientation of the end-effector.

A. Determination of the elbow position and orientation

Let $z_e \in [z_e^{min}, z_e^{max}]$ be the z-coordinate of an elbow position for a given position and orientation of the end-effector. The intersection of the ellipsoid with the plane $z = z_e$ results in a circle. The radius r_1 and the center M_1 of this circle (figure 4) are given by

$$r_1 = l_s + \sqrt{l_u^2 - z_e^2} \tag{5}$$

$$M_1 = (0,0,z_e)^T \tag{6}$$

The intersection of the sphere with the plane $z = z_e$ results in a circle. The radius r_2 and the center M_2 of this circle (figure 5) are given by

$$r_2 = l_s + \sqrt{l_f^2 - dz_e^2}, \quad dz_e = z_e - z_w \tag{7}$$

$$M_2 = (x_w, y_w, z_e)^T \tag{8}$$

The two points $\vec{e}_1$ and $\vec{e}_2$ provided by the intersection of the circles represent two possible positions of the elbow. In addition, the unit vectors of the frame (x_4, y_4, z_4) attached to the elbow must be established. The vector $\vec{z}_4$ lies along the forearm and points to the wrist. The vector $\vec{y}_4$ is perpendicular to the upperarm ($\vec{r}_u$) and forearm ($\vec{r}_f$). The vector $\vec{x}_4$ completes the right-handed coordinate frame.

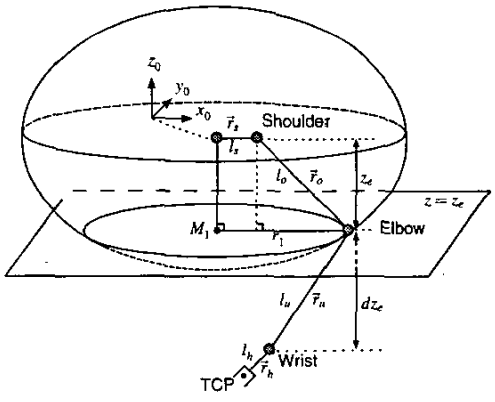

Fig. 4. The Ellipsoid and the plane $z = z_e$

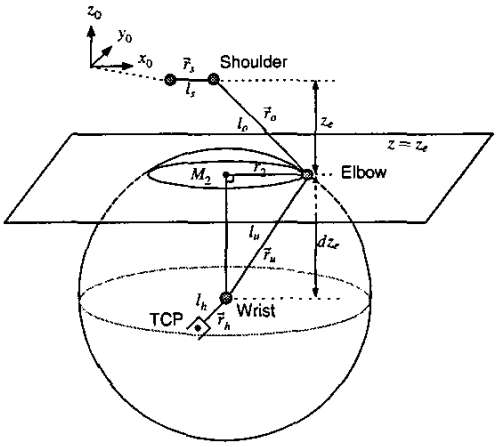

Fig. 5. The Sphere and the plane $z = z_e$

The above criteria can be formally expressed as:

$$\vec{z}_4 = \frac{\vec{r}_u}{\|\vec{r}_u\|}$$

$$\vec{y}_4 = \frac{\vec{z}_4 \times \vec{r}_o}{\|\vec{z}_4 \times \vec{r}_o\|}$$

$$\vec{x}_4 = \vec{y}_4 \times \vec{z}_4$$

The vectors $\vec{r}_u$ and $\vec{r}_o$ can be expressed using the vector $\vec{w}$ from equation (4), the elbow position vectors $\vec{e}_{1,2}$ and the position vector of the shoulder $\vec{r}_s$:

$$\vec{z}_4 = \frac{\vec{w} - \vec{e}_i}{\|\vec{w} - \vec{e}_i\|} \tag{9}$$

$$\vec{y}_4 = \frac{\vec{z}_4 \times (\vec{r}_s - \vec{e}_i)}{\|\vec{z}_4 \times (\vec{r}_s - \vec{e}_i)\|} \qquad i = 1,2 \tag{10}$$

$$\vec{x}_4 = \vec{y}_4 \times \vec{z}_4 \tag{11}$$

Having determined the position and the unit vectors of the frame attached to the elbow, the two possible positions of the elbow can be expressed by the homogeneous transformation matrix

$$T_{elbow} = \begin{pmatrix} \vec{x}_4 & \vec{y}_4 & \vec{z}_4 & \vec{e}_i \\ 0 & 0 & 0 & 1 \end{pmatrix} \qquad i = 1,2 \tag{12}$$

which provides the position and orientation of the (x_4, y_4, z_4) with respect to the base frame.

In order to get z_e^{min} and z_e^{max}, we consider the necessary but not sufficient condition, which a point of intersection of the circles mentioned above must satisfy

$$\sqrt{x_w^2 + y_w^2} \leq r_1 + r_2 \tag{13}$$

and substitute r_1 from equation (5) and r_2 from equation (7) in equation (13) and solve for z.

B. Solution of the inverse kinematics problem

The task of solving the inverse kinematics problem results in the determination of the arm joint angles for a given position and orientation of the end effector. The relationship between the elbow and the reference base frame is given by equation (12). Furthermore, this relationship can be expressed as

$$T_{elbow} = A_1 \cdot A_2 \cdot A_3 \cdot A_4 \tag{14}$$
$$= \begin{pmatrix} n'_x & o'_x & a'_x & p'_x \\ n'_y & o'_y & a'_y & p'_y \\ n'_z & o'_z & a'_z & p'_z \\ 0 & 0 & 0 & 1 \end{pmatrix}$$

Note that the expression of the position and orientation of the frame (x_4, y_4, z_4) depends only on the first four joint variables $\theta_1, \theta_2, \theta_3$ and θ_4, which are responsible for the position of the wrist. The position and orientation of the end-effector relative to the elbow is given by

$$T'' = A_4^{-1} \cdot A_3^{-1} \cdot A_2^{-1} \cdot A_1^{-1} \cdot T_{elbow} \tag{15}$$
$$= A_5 \cdot A_6 \cdot A_7 = \begin{pmatrix} n''_x & o''_x & a''_x & p''_x \\ n''_y & o''_y & a''_y & p''_y \\ n''_z & o''_z & a''_z & p''_z \\ 0 & 0 & 0 & 1 \end{pmatrix}$$

Hence, the inverse kinematics problem can be decomposed into two smaller dimension subproblems: the inverse kinematics problem given by equation (14) and the inverse kinematics problem given by equation (15). The solution starts with the matrix equation

$$\underbrace{A_1^{-1} \cdot T_{elbow}}_{L_1} = \underbrace{A_2 \cdot A_3 \cdot A_4}_{R_1} \tag{16}$$

To simplify the notation s_i and c_i are $\sin\theta_i$ and $\cos\theta_i$, respectively. The notation $W(i,j)$ denotes the element of the ith row and jth column of the matrix W. The equation $L_1(3,4) = R_1(3,4)$ of the elements of the matrices L_1 and R_1 can be used to solve for θ_1. This yields:

$$\theta_{1_{1,2}} = \text{atan2}\ (\pm p'_y, \pm p'_x) \tag{17}$$

The equations $L_1(1,4) = R_1(1,4)$ and $L_1(2,4) = R_1(2,4)$ of the matrices L_1 and R_1 provide the solution for θ_2:

$$\theta_2 = \text{atan2}\ (-p'_z, c_1 p'_x + s_1 p'_y - l_s) \tag{18}$$

The solution for the joint angles θ_3 and θ_4 can be obtained from the following matrix equation:

$$\underbrace{A_2^{-1} \cdot A_1^{-1} \cdot T_{elbow}}_{L_2} = \underbrace{A_3 \cdot A_4}_{R_2} \tag{19}$$

The equations $L_2(1,2) = R_2(1,2)$ and $L_2(2,2) = R_2(2,2)$ of the elements of the matrices L_2 and R_2 provide θ_3 as follows:

$$\theta_3 = \text{atan2}\ (-s_1 o'_x + c_1 o'_y, \quad -s_2 c_1 o'_x - s_2 s_1 o'_y - c_2 o'_z) \tag{20}$$

The equations $L_2(3,1) = R_2(3,1)$ and $L_2(3,3) = R_2(3,3)$ of the elements of the matrices L_2 and R_2 provide θ_4 as follows:

$$\theta_4 = \text{atan2}\ (c_2 c_1 n'_x + c_2 s_1 n'_y - s_2 n'_z, \quad c_2 c_1 a'_x + c_2 s_1 a'_y - s_2 a'_z) \tag{21}$$

Since the joint angles $\theta_1, \theta_2, \theta_3$ and θ_4 are already known, closed-form expressions for the joint variables θ_5, θ_6 and θ_7 can be obtained from the matrix equation:

$$\underbrace{A_5^{-1} \cdot T''}_{L_3} = \underbrace{A_6 \cdot A_7}_{R_3} \tag{22}$$

The equation $L_3(3,2) = R(3,2)$ of the elements of the matrices L_3 and R_3 can be used to solve for θ_5. This yields:

$$\theta_{5_{1,2}} = \text{atan2}\ (\pm o''_y, \pm o''_x) \tag{23}$$

The equations $L_3(1,2) = R_3(1,2)$ and $L_3(2,2) = R_3(2,2)$ of the elements of the matrices L_3 and R_3 provide θ_6 as follows:

$$\theta_6 = \text{atan2}\ (-o''_z, -c_5 o''_x - s_5 o''_y) \tag{24}$$

Solving the equations $L_3(3,1) = R_3(3,1)$ and $L_3(3,3) = R_3(3,3)$ for the joint angle θ_7 then yields:

$$\theta_7 = \text{atan2}\ (-s_5 n''_x + c_5 n''_y, s_5 a''_x - c_5 a''_y) \tag{25}$$

In the follwoing section we describe how to select a human-like arm configuration out of the infinite number of distinct possible ones.

IV. HUMAN-LIKE ROBOT ARM MOTION

The underlying idea for the generation of human-like robot arm motions is based on the results in [12] and [13]. Soechting and Flanders have shown that arm movements are planned in shoulder-centered spherical coordinates and suggest a sensorimotor transformation model that maps the wrist position on a natural arm posture using a set of representation parameters q_e^u, q_e^f, q_y^u and q_y^f, which are the upperarm elevation, the forearm elevation, the upperarm yaw and the forearm yaw, respectively (figure 7).

The relation between these parameters and the spherical coordinates of the wrist position r, ϕ and χ is given by

$$\begin{aligned} q_e^u &= -4.0 + 1.10\, r + 0.90\, \phi \\ q_e^f &= 39.4 + 0.54\, r - 1.06\, \phi \\ q_y^u &= 13.2 + 0.86\, \chi + 0.11\, \phi \\ q_y^f &= -10.0 + 1.08\, \chi - 0.35\, \phi \end{aligned} \tag{26}$$

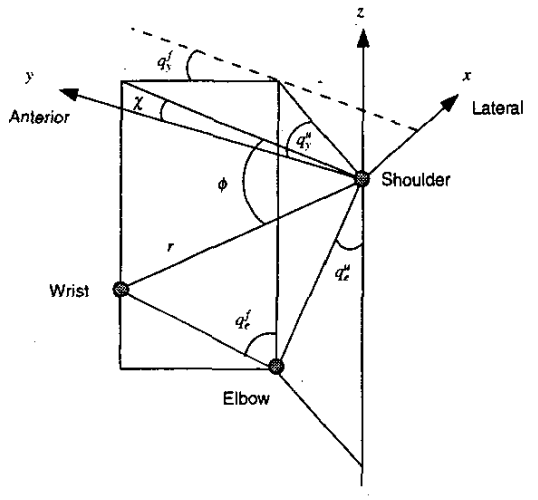

Fig. 6. Parameters for the human arm posture

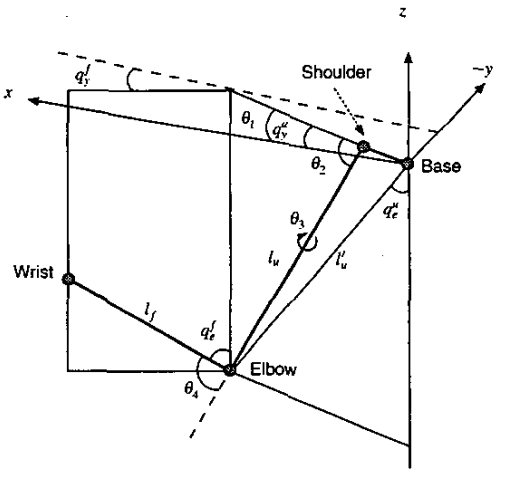

Fig. 7. Parameters for the humanoid arm posture.

Once these parameters are obtained for a given position of the wrist frame, they are mapped on the joint angles of the shoulder and elbow θ_1, θ_2, θ_3, and θ_4 of the robot arm. Note that the position of the wrist is completely determined by these angles. The joint angles θ_1 and θ_2 depend only on the upperarm elevation q_e^o and forearm yaw q_e^f.

$$\theta_1 = -q_y^u \tag{27}$$

$$\theta_2 = \pi - q_e^u - \arccos\left(\frac{l_s \cdot \cos(q_e^u)}{l_u}\right) \tag{28}$$

The joint angle θ_4 can be determined from the scalar product of $\vec{l}_u$ and $\vec{l}_f$. This yields:

$$\theta_4 = \pm\arccos\left(\frac{<\vec{l}_u, \vec{l}_f>}{||\vec{l}_u|| \cdot ||\vec{l}_f||}\right) \tag{29}$$

$$= \pm\arccos\Big(\cos(\theta_2)\cdot\sin(q_y^u)\cdot\sin(q_e^f)\cdot\sin(q_y^f) + \cos(\theta_2)\cdot\cos(q_y^u)\cdot\sin(q_e^f)\cdot\cos(q_y^f) - \sin(\theta_2)\cdot\cos(q_e^f)\Big)$$

The difference $(z_e - z_w)$ of the wrist and elbow z-coordinate can be determined using the direct kinematics and the arm representation parameters. Thus, the joint angle θ_3 can be computed as follows:

$$\theta_3 = \arcsin\left(\frac{\sin(\theta_2)\cdot\cos(\theta_4)+\cos(q_e^f)}{\cos(\theta_2)\cdot\sin(\theta_4)}\right) \tag{30}$$

Since the sensorimotor transformation model is only an approximation, the wrist position given by the determined angles θ_1, θ_2, θ_3 and θ_4 does not exactly concide with the target one. However, the exact position and orientation of the end-effector can be reached by applying the inverse kinematics algorithm presented in section III-B, which allows calculating the remaining joint angles θ_5, θ_6 and θ_7. In case one of these angles violates its limit, we correct this by changing iteratively the elbow position until either a feasible solution is found or all possible positions of the elbow in the interval $[z_e^{min}, z_e^{max}]$ are exhausted.

V. Results and Conclusions

The generation of human-like manipulation motions has been implemented and tested successfully for the 7-DOF arm of the humanoid robot ARMAR. The result is a real-time control scheme that eliminates a major part of unnatural arm configurations during the execution of manipulation tasks. Figure 8 shows an example of the desired (dushed line) and generated (solid line) position trajectories in the Cartesian space during the execution of a manipulation task operation. The deviations are compensated through the inverse kinematics algorithm with minimal modifications of the joint angle trajectories determined according to section IV.

The presented approach does not consider the dynamics of the robot arm. This would be necessary to generate realistic velocity distribution for manipulation motions. A limitation of the proposed way to generate human-like motions is the simple kinematic structure of the robot arm. In the case of complex manipulation tasks, the exact position and orientation of the hand can be obtained only through significantly large modifications of the joints θ_1, θ_2, θ_3 and θ_4. However, the resulting configuration ist not guaranteed to be human-like. Therefore, a humanoid robot arm with a higher degree of redundancy is envisaged.

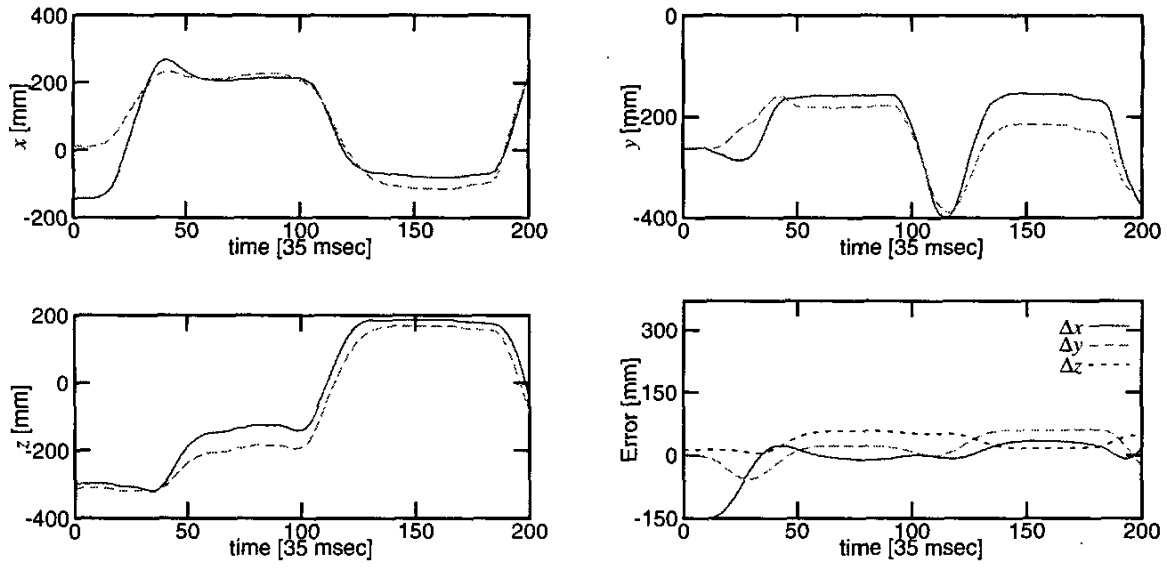

Fig. 8. Time history of the position trajectories.

VI. ACKNOWLEDGMENTS

This work has been performed in the framework of the german humanoid robotics program SFB 588 funded by the *Deutsche Forschungsgemeinschaft (DFG).*

VII. REFERENCES

[1] M. Benati, S. Gaglio, P. Morasso, V. Tagliassco, and R. Zaccaria. Anthropomorphic Robotics: I. Representing Mechanical Complexity. *Biological Cybernetics*, 38:125–140, 1980.

[2] A. Ligeois. Automatic Supervisory Control of the Configuration and Behavior of Multibody Mechanism. *IEEE Transaction on Systems, Man and Cybernetics*, 1977.

[3] A.A. Maciejewski and C.A. Klein. Obstacle Avoidance for Kinematically Redundant Manipulators in Dynamically Varying Environments. *The International Journal of Robotics Research*, 4(3):109–117, 1985.

[4] Y. Nakamura and H. Hanafusa. Inverse Kinematics Solution with Singularity Robustness for Robot Manipulator Control. *ASME Journal of Mechanisms, Transmissions, Automation, Design*, 108:163–171, 1986.

[5] K.N. Groom, A.A. Maciejewski, and V. Balakrishnan. Real-Time Failure-Tolerant Control of Kinematically Redundant Manipulators. *The International Conference on Robotics and Automation*, pages 2595–2600, 1997.

[6] J.M. Hollerbach and K.C. Suh. Redundancy Resolution of Manipulators through Torque Optimization. In *IEEE International Conference on Robotics and Automation (ICRA)*, volume 4, pages 308–316, 1987.

[7] Y. Nakamura. *Advanced Robotics: Redundancy and Optimization*. Addison Wesley Publishing, 1991.

[8] H. Cruse, E. Wischmeyer, M. Brüwer, P. Brockfeld, and A. Dress. On the Cost Funktions for the Control of the Human Arm Movement. *Biological Cybernetics*, 62:519–528, 1990.

[9] V. Potkonjak, M. Popovic, M. Lazarevic, and J. Sinanovic. Redundancy Problem in Writing: From Human to Anthropomorphic Robot Arm. *IEEE Transactions on Systems, Man and Cybernetics (Part B: Cybernetics)*, 28(6):790–804, 1998.

[10] A. Ude, C. Man, M. Riley, and C.G. Atkeson. Automatic Generation of Kinematic Models for the Conversion of Human Motion Capture Data into Humanoid Robot Motion. In *Proceeding of the First IEEE-RAS International Conference on Humanoid Robots*, pages 2223–2228, Boston, 2000.

[11] T. Asfour, A. Ude, K. Berns, and R. Dillmann. Control of ARMAR for the Realization of Anthropomorphic Motion Patterns. In *The 2nd IEEE-RAS International Conference on Humanoid Robots (HUMANOIDS 2001)*, Tokyo, Japan, 2001.

[12] J. F. Soechting and M. Flanders. Sensorimotor Representations for Pointing to Targets in Three-Dimensional Space. *Journal of Neurophysiology*, 62(2):582–594, 1989.

[13] J. F. Soechting and M. Flanders. Errors in Pointing are Due to Approximations in Targets in Sensorimotor Transformations. *Journal of Neurophysiology*, 62(2):595–608, 1989.